https://doi.org/10.3311/PPee.39509



Periodica Polytechnica Electrical Engineering and Computer Science

# Experimental Verification of a Fuzzy Adaptive Sliding Mode Control Design for IM Speed Control

Boudjema Sabouni[1], Khadidja Makhloufi[1], Mokhtar Zerikat[2], Bousmaha Bouchiba[1*], Ismail Khalil Bousserhane[1]

[1] Smart Grids and Renewable Energies Laboratory, University Tahri Mohamed of Bachar, P. O. B. 417, 08000 Bechar, Algeria
[2] Laboratory of Automation and System Analysis (LAAS), Ecole Nationale Polytechnique d'Oran Maurice Audin, P. O. B. 1523, El M'Naouer, 31000 Oran, Algeria
[*] Corresponding author, e-mail: bouchiba.bousmaha@univ-bechar.dz

Received: 07 December 2024, Accepted: 26 May 2025, Published online: 27 June 2025

**Abstract**

This article aims to develop a fuzzy adaptive SMC technique that incorporates a variable boundary layer and adaptive switching gain for speed control of a three-phase induction motor (IM) drive. The boundary-layer characteristics are chosen to offer the best compromise between control robustness and chattering elimination or reduction. In addition, this technique offers many advantages for uncertain dynamic systems. The chattering phenomenon, a well-known problem in classical SMC, arises when the switching function attracts the state trajectory toward the sliding surface. Several methods and approaches have been tried to eliminate this phenomenon. We propose here an approach that involves fuzzy logic to avoid this undesirable effect so that the stability condition according to Lyapunov is verified. This fuzzy adaptation system associated with the SMC (FASMC) towards the obtained results forms a robust tool for chattering reduction. Finally, an experimental prototype setup tests the robustness of the fully developed control structure. The experimental results obtained from the FASMC for speed IM drives demonstrate the highest effectiveness and robustness when compared to the conventional SMC controller.

**Keywords**

induction motor, classical sliding mode control, adaptive sliding mode, fuzzy logic adaptation system, variable boundary layer thickness, variable switching gain

## 1 Introduction

In recent years, significant development and considerable technological advances, both in power electronics and microelectronics, have brought considerable progress in AC machine application and robust controls' real-time implementation. The induction motors (IMs) have been used for numerous industrial applications due to their simplicity of design, low maintenance cost, high efficiency, and reliability [1–3]. However, in general, their control is considerably more complex because their model is highly nonlinear, and some electrical variables cannot be directly measured, such as flux and motor parameters, especially the rotor resistance, which are often precisely unknown or time-varying. On the other hand, separately excited direct current machines were used for a long time in adjustable speed processes because their torque and flux are naturally decoupled and can be easily controlled [1, 2, 4, 5].

High-performance induction motor drives frequently adopt the field-oriented control strategy. This control strategy provides decoupling of the flux and torque control signals of the induction motor, so its dynamic behavior is quite similar to that of a separately excited DC motor [1, 3–7]. Usually in a vector control approach, the use of classical proportional-integrator (PI) regulators to implement the *d-q* axis currents and speed control loops of the IM is the most frequent case, due to their structural simplicity and acceptable control performances in a wide range of operating conditions [6, 7]. However, these classical controllers are still inadequate when the process dynamics are highly nonlinear and precise performances are required. Also, vector control's performance is affected by motor parameter uncertainties and unpredictably changing external loads. Because of this, it is not possible to achieve exact decoupling control between torque and flux [4, 6, 7].

These technical and technological advantages have oriented the research community toward advanced techniques

**Cite this article as:** Sabouni, B., Makhloufi, K., Zerikat, M., Bouchiba, B., Bousserhane, I. K. "Experimental Verification of a Fuzzy Adaptive Sliding Mode Control Design for IM Speed Control", Periodica Polytechnica Electrical Engineering and Computer Science, 2025. https://doi.org/10.3311/PPee.39509

to deal with internal parameter variations and external load changes. For example, exact feedback linearization, backstepping, sliding mode control, and adaptive control have been successfully implemented for the IM drive [8–11]. One of these advanced strategies, sliding mode control (SMC), has garnered significant attention for its robustness against uncertainties and its ability to provide good robustness, stability, and fast dynamic responses [9–16]. This control strategy employs a discontinuous switching control action, initially pushing the system's variable states towards a sliding surface, and subsequently guiding them along this surface towards an equilibrium point. It can operate some nonlinear systems that are not primarily stable using linear controllers [12–16]. However, due to its switching nature, it presents numerous operating limits in electrical drives and induces high-frequency oscillations known as chattering characteristics. This phenomenon results in several undesirable effects, including harmonics, torque pulsation, system control instability, and damage to the controller's elements [12].

Notwithstanding the benefits of the SMC technique, addressing the chattering phenomenon poses a significant challenge. The use of the functions called soft has made it possible, where the basic idea is to be based on the combination of artificial intelligence and classical SMC, especially fuzzy logic and other advanced techniques [8–11, 17–24]. The purpose of fuzzy logic is the study and representation of imprecise knowledge and approximate reasoning. As a result, the used fuzzy logic system will generate an adaptive factor that can adjust the parameters or compensate for the variations of the discontinuous function, offering a compromise between robustness, precision, and the elimination of chattering. Thus, the large success of fuzzy logic control is due to its ability to translate a skilled operator's control strategy into a set of easily interpretable linguistic rules [11, 17–20].

Several hybrid methods, including fuzzy logic, neural networks, and genetic algorithms, integrate classical sliding mode control, adaptive control, and artificial intelligence to maintain control robustness and minimize chattering stress [9–11, 17–30]. Amieur et al. [18] have proposed a design of a fuzzy sliding mode controller with an adjustable gain for a nonlinear multi-input multi-output system. Amieur et al. [18] suggested a way to solve the problem of not having a way to figure out the gain $k$ in the SMC. It is based on an adaptive method, and its design is created using Lyapunov stability. In [19], a robust sliding mode controller with an adaptive switching gain and integrator has been designed to decrease the effects of uncertainties and external disturbance. The development of a hybrid fuzzy sliding mode controller has been investigated in [21] for robust control of both active/reactive power in the DFIG for WECS applications. The controller designed by [21] has the objective of suppressing the chattering stresses/values and ensuring robustness and precision against disturbance variation. Itouchene et al. [22] have implemented various types of controllers based on sliding mode control design. The studied controllers are high-order SMC control and variable gain high-order SMC using super-twisting algorithms, which are all applied to enhance the control of transmitted stator active/reactive power. In [23], a fuzzy adaptive SMC controller has been applied for an electro-hydraulic position system to improve trajectory tracking precision, effectiveness, and chattering elimination. In this controller, a nonlinear integral term has been added to design the sliding surface, and an adaptive term is developed to replace the equivalent control action. A neuro-fuzzy estimator with variable gain combined with sliding mode control to suppress undesirable chattering problems and compensate the uncertainties' model can be found in [24].

In [25], another fuzzy logic regulator combined with sliding mode control was investigated for robot manipulators, demonstrating performance improvements, quick responses, convergence, higher precision, and better effectiveness. Aichi and Kendouci [26] have proposed a hybrid controller based on SMC combined with PI-Anti-Windup in which a linear supervisor is used to activate the above controllers regarding operating conditions. Furthermore, in [20] a hybrid controller combining the fuzzy logic supervisor and super-twisting second-order SMC has been designed in which the gains of STSMC are adjusted with a fuzzy system. Yang et al. [27] investigated an adaptive fuzzy sliding mode controller for an islanded inverter microgrid to improve power supply performances and deal with uncertainties without chattering effects. Furthermore, the Boukhalfa et al. [31] proposed a novel genetic algorithm-optimized fuzzy second-order sliding mode control (G-FSOSMC) for direct torque control of dual star induction motors (DTC-DSIM) to reduce torque/flux ripples, chattering, and sensitivity to parametric variations. Baek et al. [32] introduced a novel adaptive sliding mode control (ASMC) employing a designed adaptive law to adjust the switching control gains near the sliding surface. The proposed method by [32] addresses drawbacks of classical SMC, such as chattering and excessive gains adaptation, by ensuring quick and strategic reduction of switching gains

near the sliding surface. Sacchi et al. [33] introduced a neural network-based integral sliding mode (NN-ISM) control for nonlinear systems with uncertain drift terms and control effectiveness matrices, leveraging deep neural networks to approximate unknown system dynamics and design the integral sliding manifold, ensuring ultimate boundedness of the system state through Lyapunov stability analysis. Another approach has been proposed by Roy et al. [34] that treats a significant gap in the field of adaptive sliding mode control design, where a novel methodology that does not require a priori knowledge bounds uncertainty. An adaptive chattering-free terminal sliding-mode control (TSMC) method designed for *n*-order nonlinear systems with unknown disturbances and model uncertainties can be found in [35]. The proposed method leverages finite-time convergence to address the singularity problem and ensure robustness against system uncertainties and disturbances. In [36], a hybrid fuzzy logic-based sliding mode control optimized by the imperialist competitive algorithm for energy management in multi-area power systems with wind power generation has been proposed, effectively stabilizing frequency and tie-line power deviations. Another hybrid controller based on a fuzzy adaptive PID fast terminal sliding mode control technique for redundant manipulators has been presented to improve accurate tracking performance and suppress the chattering problem [37]. A neuro-fuzzy adaptive SMC for quad-rotor, combining classical SMC with ANN and fuzzy logic control, has been developed to address chattering attenuation and unmatched/matched uncertainties [38]. Furthermore, other approaches based on adaptive sliding mode control applications for nonlinear systems can be found in [39–42].

Motivated by the advantages of previous studies, this research employs an adaptive fuzzy logic controller to instantaneously adjust the coefficients, both gain and boundary layer thickness, of the discontinuous switching term. This adjustment is based on an appropriate intelligent mechanism, and its goal is to improve control performance when parameters change and external loads are applied. This study can represent a powerful solution to the problems induced by the chattering phenomenon, find the compromise between the tracking error and the boundary layer thickness, and allow the controller to achieve a smoother control signal. Generally, we can summarize the main objectives of this study as follows:

- A detailed mathematical design procedure of speed and current controllers based on indirect field-oriented IM control is presented.
- The sliding mode control problems are avoided using adjusted switching control parameters, solving the trade-off between them by employing a fuzzy logic adaptation system.
- The switching function gains are tuned instantaneously using a fuzzy logic adaptation system designed in a simplified way according to the transient and steady-state conditions of system state locations relative to the sliding surfaces.
- By employing the decision-making capability of the FLC to instantly learn the switching control parameters, the prior knowledge of upper limit uncertainty is suppressed, leading to enhanced high dynamic performance stability and also effectively mitigating the chattering problem caused by excessive large gain selection.
- The successful real-time implementation of the FASMC for IM speed drive in the dSPACE DS114 board in order to show the superiority of the proposed controller.

This paper investigates the design of a fuzzy adaptive sliding mode controller (FASMC) for IM speed control, focusing on indirect field orientation. Classical SMC controllers are used for current control loops that yield satisfactory tracking of steady-state and transient-state performances. In the outer speed control loop, a fuzzy adaptive SMC controller was developed to achieve high control responses and considerably reduce the chattering problem while ensuring stability and robustness and improving the motor's performance. The rest of the paper is organized as follows: The model and indirect field-oriented control of the IM drive system are described in Section 2. The control design of the sliding mode controller for IM speed/currents control is developed and presented in Section 3. Section 4 then elaborates on the proposed FASMC for IM speed control. The experimental result using dSPACE 1104 of the proposed controller design is defined in Section 5. Section 6 draws some final conclusions.

## 2 Indirect field oriented control of an induction motor

The dynamic model of the three-phase *Y*-connected induction motor can be written in the *d-q* synchronous frame by the following differential equations [1, 4, 7, 19, 28–30, 43].

$$i_{ds} = \frac{1}{\sigma L_s}\left(-R_{eq} i_{ds} + \sigma L_s \omega_s i_{qs} + \frac{L_m R_r}{L_r^2}\varphi_{dr} + \frac{pL_m}{L_r}\varphi_{qr}\omega_r + v_{ds}\right) \tag{1}$$

$$i_{qs} = \frac{1}{\sigma L_s}\left(-\sigma L_s \omega_s i_{ds} - R_{eq} i_{qs} - \frac{pL_m}{L_r}\omega_r \varphi_{dr} + \frac{L_m R_r}{L_r^2}\varphi_{qr} + v_{qs}\right) \tag{2}$$

$$\dot{\varphi}_{dr} = \frac{L_m R_r}{L_r} i_{ds} - \frac{R_r}{L_r}\varphi_{dr} + \left(\omega_s - p\omega_r\right)\varphi_{qr} \tag{3}$$

$$\dot{\varphi}_{qr} = \frac{L_m R_r}{L_r} i_{qs} - \left(\omega_s - p\omega_r\right)\varphi_{dr} - \frac{R_r}{L_r}\varphi_{dr} \tag{4}$$

$$\dot{\omega}_r = \frac{1}{J}\left(\frac{3}{2}\frac{PL_m}{L_r}\left(i_{qs}\varphi_{dr} - i_{ds}\varphi_{qr}\right) - f_c\omega_r - T_l\right) \tag{5}$$

Where $R_s$ and $R_r$ denote the stator and rotor resistance per phase, $L_m$ is the magnetizing inductance per phase. $L_s$ and $L_r$ are the stator inductance and rotor inductance per phase, respectively; $\omega_s$ denotes the synchronous frequency, $\omega_r$ is the rotor frequency, $p$ is the number of pole pairs, $\tau_r = L_r/R_r$ is the rotor time constant, $\sigma = 1 - L_m^2/L_s L_r$ represents the leakage coefficient, $i_{ds}$ and $i_{qs}$ are the $d$-axis and $q$-axis stator current, $\varphi_{dr}$ and $\varphi_{qr}$ are the $d$-axis and $q$-axis rotor flux, and $v_{ds}$ and $v_{qs}$ are the $d$-axis and $q$-axis stator voltage, respectively and $R_{eq} = R_s + (L_m/L_r)^2 R_r$. The electromagnetic torque can be written as follows [1, 2, 6, 7]:

$$T_e = \frac{3}{2}\frac{PL_m}{L_r}\left(i_{qs}\varphi_{dr} - i_{ds}\varphi_{qr}\right). \tag{6}$$

The behavior of the induction motor with vector control can be shown as a separately excited DC machine where its torque and flux are independently controlled [7]. If the rotor field orientation is completely ensured, the quadratic rotor flux $\varphi_{qr}$ is set to equal zero, then we can write:

$$\varphi_{qr} = 0 \tag{7}$$

$$\varphi_{qr} = \varphi_r^N = \text{constant}, \tag{8}$$

where $\varphi_r^N$ denotes the rotor flux rated value.

As a result, we simplify the torque equation to resemble the torque equation of a DC motor, as shown in [6, 7].

$$T_e = \frac{3}{2}\frac{PL_m}{L_r} i_{qs}\varphi_{dr} \tag{9}$$

And the slip frequency, $\omega_{sl} = \omega_s - p\omega_r$, is computed by Eq. (10):

$$\omega_{sl} = \frac{1}{\tau_r}\frac{i_{qs}^*}{i_{ds}^*}, \tag{10}$$

where the superscript "*" represents reference values.

## 3 Sliding mode control design for IM drive

The sliding mode control is a type of variable structure control. It is well known as an effective strategy of robust controller design for a variety of complex nonlinear systems that operate under various uncertain conditions [12–15]. It has many incontestable advantages, such as robustness against external disturbances, precision, stability, and insensitivity to parameter variations of the controlled system. Due to these advantages, the SMC has become a popular technical solution for different scientific and technological areas such as electric drives, robotics, nonlinear process control, and vehicles [11, 12, 17–19, 23–28]. The SMC objective is to conduct system state trajectories to a defined sliding surface and then maintain them around this surface using an appropriate switching control law. The sliding surface can be expressed as [13]:

$$s(x) = \left(\frac{\partial}{\partial t} + \lambda\right)^{n-1} e(x), \tag{11}$$

where $x$ denotes the controlled variable, $\lambda$ is a positive constant, and $n$ is the order of the system.

The general structure of the sliding mode controller is composed of two parts: one concerns the system's exact linearization ($u_{eq}$) and the second is for system stabilization, $u_n$ [11, 13, 19, 28].

$$u = u_{eq} + u_n \tag{12}$$

The $u_{eq}$ represents the equivalent control action that ensures the system states remain on the sliding surface, while $u_n$ refers to the discontinuous switching control action that mitigates the effects of uncertainties, as provided by [19]

$$u_n = k \cdot \text{sgn}\left(s(x)\right), \tag{13}$$

where $k$ is positive design constant.

However, classical SMC law presents the chattering problem. The most popular solution to this problem involves replacing the sgn(·) function with a smooth function, such as saturation (sat(·)), hyperbolic tangent function, or a tangent-sigmoid switching function. Consequently, the discontinuous switching control action can be defined as [11, 12, 28]

$$u_n = k \cdot \text{sat}\left(\frac{s(x)}{\xi}\right), \tag{14}$$

where $\xi$ denotes the boundary layer thickness.

And the saturation function is defined as:

$$\text{sat}(\phi) = \begin{cases} \phi & \text{if } |\phi| < 1 \\ \text{sgn}(\phi) & \text{if } |\phi| \geq 1 \end{cases}. \tag{15}$$

### 3.1 Sliding mode speed controller design

The main objective of SMC design is to create a control law that ensures a finite-time convergence of motor speeds with good dynamic performance. In order to achieve this objective, a tracking error has been derived for choosing the switching surface as follows:

$$e_\omega = \omega_r^* - \omega_r, \tag{16}$$

where $\omega_r^*$ represents the desired speed.

Then, the sliding surface can be defined according to Eq. (11), taking $n = 1$, as follows:

$$s_\omega = \omega_r^* - \omega_r. \tag{17}$$

Differentiating Eq. (17) gives:

$$\dot{s}_\omega = \dot{\omega}_r^* - \dot{\omega}_r = \dot{\omega}_r^* - \left( \frac{3pL_m}{2L_r} i_{qs} \varphi_{dr} - f_c \omega_r - T_l \right) \Big/ J. \tag{18}$$

Choosing an adopted Lyapunov function for a control system using SMC is done as follows:

$$V_1 = \frac{1}{2} s_\omega^2. \tag{19}$$

The derivative of Eq. (19) gives

$$\dot{V}_1 = s_\omega \cdot \dot{s}_\omega. \tag{20}$$

Taking into consideration Eq. (18), Eq. (20) can be written as

$$\dot{V}_1 = s_\omega \left( \dot{\omega}_r^* - \left( \frac{3PL_m}{2L_r} i_{qs} \varphi_{dr} - f_c \omega_r - T_l \right) \Big/ J \right). \tag{21}$$

According to Eq. (12), the sliding mode control law design includes two parts as

$$i_{qs}^* = i_{qs}^{eq} + i_{qs}^n. \tag{22}$$

During the sliding mode, the system state trajectory is oriented and keeps around the switching surface, i.e., $s_\omega = \dot{s}_\omega = 0$, then the equivalent control part $i_{qs}^n$ is derived:

$$i_{qs}^{eq} = \frac{2}{3} \frac{JL_r}{PL_m \varphi_{dr}} \left( \dot{\omega}_r^* + \frac{f_c}{J} \omega_r + \frac{T_l}{J} \right). \tag{23}$$

And the discontinuous switching control input of the SMC can be adopted as

$$i_{qs}^n = k_\omega \cdot \mathrm{sat}\left( s_\omega / \xi_\omega \right), \tag{24}$$

where $k_\omega$ is a positive design constant.

Substituting Eq. (23) and Eq. (24) into Eq. (21) yields

$$\dot{V}_1 = s_\omega \left( -\frac{2}{3} \frac{JL_r}{pL_m} k_\omega \, \mathrm{sat}\left( s_\omega / \xi_\omega \right) \right) = -\mu_\omega \left| s_\omega \right| \le 0, \tag{25}$$

where $|s_\omega| > \xi_\omega$ and $\mu_\omega$ is a positive gain. This ensures that the system remains stable and that the speed error trajectory reaches the boundary layer, where $|s_\omega| \le \xi_\omega$.

### 3.2 Sliding mode current controller design

The IM drive control performances depend highly on the current controller's responses in the inner loop. So, high-accuracy current control is strongly needed to obtain good dynamic responses for FOC IM drives. In Section 3.2, the sliding mode current controller design, $i_{ds}$ and $i_{qs}$, based on indirect field-oriented is developed. To achieve this goal, two sliding surfaces are chosen as

$$s_d = i_{ds}^* - i_{ds} \tag{26}$$

$$s_q = i_{qs}^* - i_{qs}, \tag{27}$$

where $i_{ds}^*$ and $i_{qs}^*$ are the *d*- and *q*-axis reference stator currents, respectively.

The derivative of the two sliding surfaces is expressed as

$$\begin{aligned} \dot{s}_d &= i_{ds}^* - i_{ds} \\ &= i_{ds}^* - \frac{1}{\sigma L_s} \left( -R_{eq} i_{ds} + \sigma L_s \omega_s i_{qs} + \varphi_{dr} \frac{L_m R_r}{L_r^2} + v_{ds} \right) \end{aligned} \tag{28}$$

$$\begin{aligned} \dot{s}_q &= i_{qs}^* - i_{qs} \\ &= i_{qs}^* - \frac{1}{\sigma L_s} \left( -\sigma L_s \omega_s i_{ds} - R_{eq} i_{qs} - p \frac{L_m}{L_r} \varphi_{dr} \omega_r + v_{qs} \right). \end{aligned} \tag{29}$$

If the tracking errors are kept around the sliding surfaces, $s_d = s_q = 0$, $t \ge 0$ and $\dot{s}_d = \dot{s}_q = 0$. Thus, by solving the two equations $\dot{s}_d = 0$ and $\dot{s}_q = 0$, the *d*- and *q*-axis voltage equivalent control actions could be found as

$$v_{ds}^{eq} = \left( \sigma L_s i_{ds}^* + R_{eq} i_{ds} - \sigma L_s \omega_s i_{qs} - \frac{L_m R_r}{L_r^2} \varphi_{dr} \right) \tag{30}$$

$$v_{qs}^{eq} = \left( \sigma L_s i_{qs}^* + R_{eq} i_{qs} + \sigma L_s \omega_s i_{ds} + p \frac{L_m}{L_r} \omega_r \varphi_{dr} \right). \tag{31}$$

Therefore, according to Eq. (12), the reference voltage control laws that conduct the system states to move towards the defined sliding surfaces in finite time can be expressed as

$$v_{ds}^* = v_{ds}^{eq} + k_d \cdot \mathrm{sat}\left( s_d / \xi_d \right) \tag{32}$$

$$v_{qs}^* = v_{qs}^{eq} + k_q \cdot \mathrm{sat}\left( s_q / \xi_q \right). \tag{33}$$

The Lyapunov functions used to analyze the stability of the control system can be adopted as

$$V_2 = 0.5 s_d^2$$
$$V_3 = 0.5 s_q^2. \quad (34)$$

The derivatives of Eq. (34) give

$$\dot{V}_2 = s_d \cdot \dot{s}_d = s_d \left( i_{ds}^* - \frac{1}{\sigma L_s} \left( -R_{eq} i_{ds} + \sigma L_s \omega_s i_{qs} + \varphi_{dr} \frac{L_m R_r}{L_r^2} + v_{ds} \right) \right) \quad (35)$$

$$\dot{V}_3 = s_q \cdot \dot{s}_q = s_q \left( i_{qs}^* - \frac{1}{\sigma L_s} \left( -\sigma L_s \omega_s i_{ds} - R_{eq} i_{qs} - p \frac{L_m}{L_r} \varphi_{dr} \omega_r + v_{qs} \right) \right). \quad (36)$$

By substituting Eq. (32) into Eq. (35) and Eq. (33) into Eq. (36), we yield

$$\dot{V}_2 = s_d \left( -\sigma L_s k_d \, \mathrm{sat}\left( s_d / \xi_d \right) \right) = -\mu_d |s_d| \le 0 \quad (37)$$

$$\dot{V}_3 = s_q \left( -\sigma L_s k_q \, \mathrm{sat}\left( s_q / \xi_q \right) \right) = -\mu_q |s_q| \le 0, \quad (38)$$

where $|s_d| > \xi_d$, $|s_q| > \xi_q$, and $\mu_d, \mu_q$ are positive constants. Thus, it guarantees the stability of the system control verified and the convergence of current error trajectories to sliding surfaces $s_d = s_q = 0$ when $t \to \infty$.

Fig. 1 shows the control block diagram of the IM speed control using the classical sliding mode control.

## 4 Fuzzy adaptive sliding mode control (FASMC) of IM speed control

As demonstrated in Section 3, the design of the sliding mode controller becomes challenging due to the optimal selection of the switching function gains, as well as the presence of uncertainties in system parameters and unknown external disturbances. So, these gains values have a significant effect on the performance quality of the control system in transient and steady states [18, 24, 25, 27]. Therefore, while an excessive gain value can enhance the speed rise time and disturbance rejection of the IM drive, it may also exacerbate chattering issues. However, on the other side, a large boundary-layer thickness may cause precision losses and provide low tracking accuracy with minimum chattering effects. In Section 4, we propose a fuzzy adaptive sliding mode control to mitigate these issues and find a compromise between the switching control parameters. The suggested hybrid controller is mainly made up of a sliding mode control design. A fuzzy logic adaptation system (FLAS) is used as a supervisor to change the switching control parameters, gain $k_\omega$ and $\xi_\omega$, continuously and instantaneously between maximal and minimal values (i.e., $\xi_\omega^{\max}$, $k_\omega^{\max}$, $\xi_\omega^{\min}$ and $k_\omega^{\min}$) based on whether the IM drives are in a steady state or a transient state, ensuring high dynamic performance.

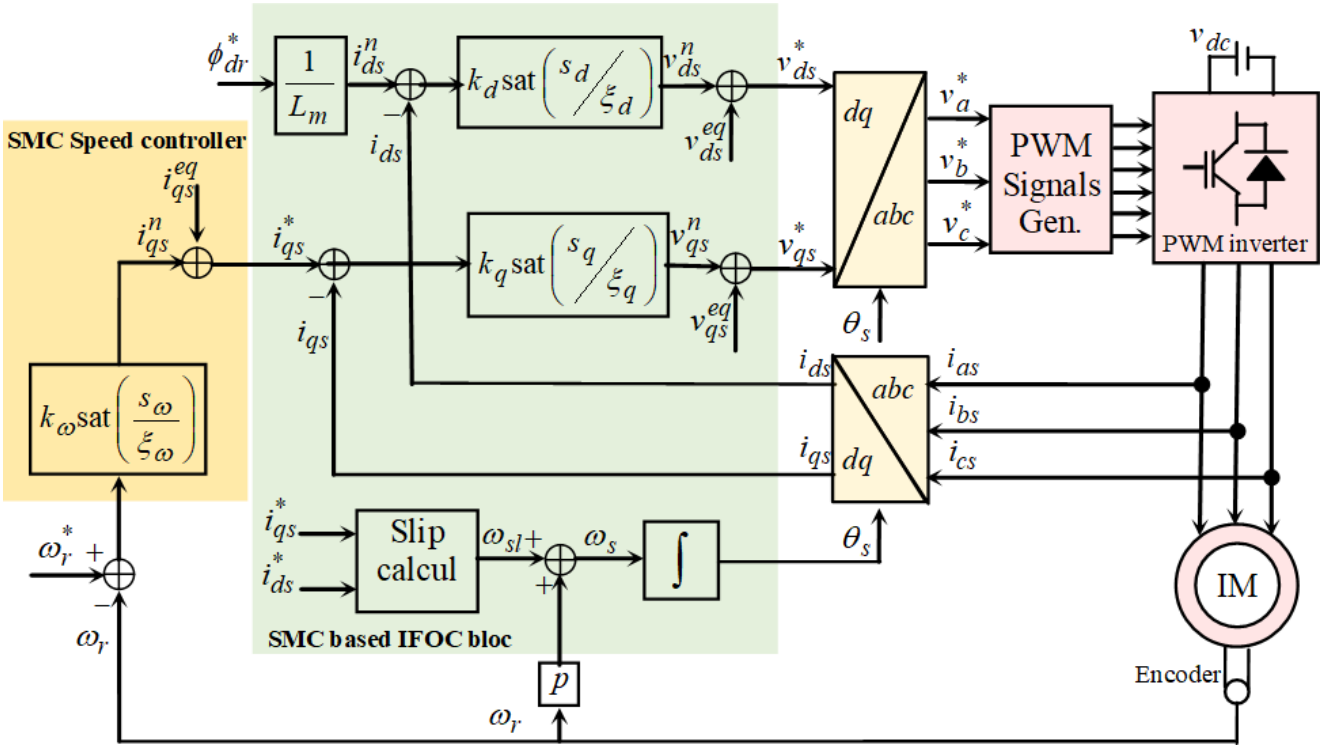


**Fig. 1** Block diagram of classical sliding mode speed and currents control

The purpose of this proposed fuzzy adaptive sliding mode control (FASMC) is to maintain the regulation performances, ensuring more robustness to the system and mainly reducing the undesirable effect of the chattering generated by the sliding mode control, which can even damage the machine and control elements. Fig. 2 shows the operating principle of the proposed adaptive sliding mode control using a fuzzy logic adaptation system. Consequently, the classical SMC speed controller's discontinuous control action (Eq. (24)) took on the following form:

$$i_{qs}^{n} = k_{\omega}^{fuz} \cdot \mathrm{sat}\left(s_{\omega} / \xi_{\omega}^{fuz}\right), \tag{39}$$

where $k_{\omega}^{fuz}$ and $\xi_{\omega}^{fuz}$ are the adjusted gain and the boundary-layer thickness of the switching control action, respectively.

In this study, we have designed a fuzzy logic adaptation system (FLAS) with two inputs and two outputs. The sliding surface $s_{\omega}$ and its derivative $\dot{s}_{\omega}$ serve as the inputs of the FLAS block, while the switching control action parameters $k_{\omega}^{fuz}$ and the boundary-layer thickness $\xi_{\omega}^{fuz}$ serve as the outputs. The main role of the FLAS block is to increase or decrease the switching discontinuous function gains instantly depending on whether the state variable is near or far from the sliding surface. The fuzzy logic adaptation system operates by reasoning that when the IM drive states and speed errors are far from the sliding surface, it should increase the switching control gains to large values. However, when the system states approach the surface, it should decrease the adaptive gains to small values. Thus, the fuzzy rule base design is based on the sliding mode reachability conditions, as follows:

- When the system's state is far from the sliding surface, $|s_{\omega}|$ is large, or moving away, i.e., $\dot{s}_{\omega}$ takes the same sign as $s_{\omega}$. The $k_{\omega}^{fuz}$ and  should be increased as much as possible to conduct the system to the sliding surface.
- When the system's state is far from the sliding surface, $|s_{\omega}|$ is large, but moving toward it, i.e., $\dot{s}$ small or taking the opposite sign of $s_{\omega}$. The $k_{\omega}^{fuz}$ and $\xi_{\omega}^{fuz}$ should be moderately increased to guarantee the convergence.
- When the system's state is close to the sliding surface, $|s_{\omega}|$ is small and approaching it. The $k_{\omega}^{fuz}$ and $\xi_{\omega}^{fuz}$ are decreased to reduce the chattering effects.
- When the system's state is on the sliding surface, $|s_{\omega}|$ is zero, and $k_{\omega}^{fuz}$ and $\xi_{\omega}^{fuz}$ are maintained as small as possible.

The fuzzy sets of inputs give us the inference rules we need to figure out how many subsets the output variable belongs to. The fuzzy logic adaptation system admits 05 fuzzy sets for each input variable: BN (big negative), MN (medium negative), Z (zero), MP (medium positive), and BP (big positive). We adopted triangular functions for each input variable, $s_{\omega}$ and $\dot{s}_{\omega}$, because of their simplicity and computational efficiency. The two FLAS outputs select only three fuzzy subset membership functions, each with a sigmoidal form and a linguistic variable defined as S (small), M (medium), and B (big). The sigmoidal functions are adopted for output variables because they can facilitate a smooth transition, ensuring gradual changes in the outputs, and guaranteeing soft tuning with precision

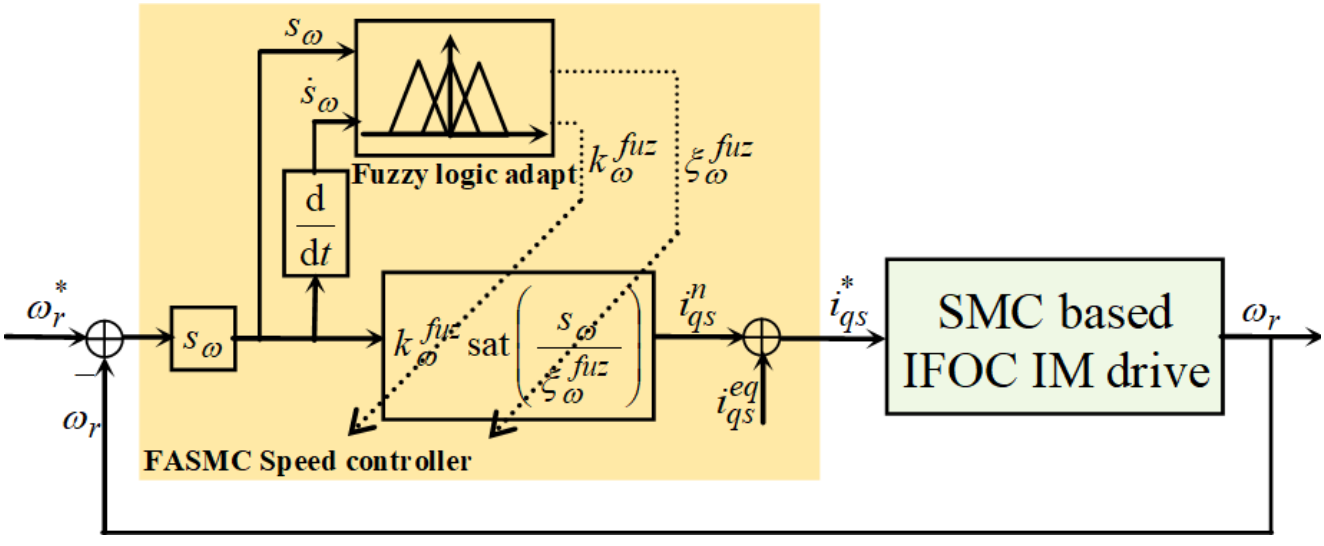


**Fig. 2** Principle of control system with FASMC

in the switching control gains. The choice of 03 linguistic terms for outputs is typically based on the fact that they offer more simplicity, provide adequate control actions, reduce the computational load (which is important for real-time systems), and simplify the rule base, making it easier for establishment and design.

The membership functions of the two inputs, $s_\omega$ and $\dot{s}_\omega$, are depicted in Fig. 3, whereas the output membership functions of the gain $k_\omega^{fuz}$ and the boundary-layer thickness $\xi_\omega^{fuz}$ are depicted in Figs. 4 and 5, respectively.

Where:

- $\xi_\omega^{\max}$, $k_\omega^{\max}$: are the maximal values possible of switching control gains
- $\xi_\omega^{\min}$ and $k_\omega^{\min}$: are the minimal values possible of switching control law gains.

With a careful and successful selection of $\xi_\omega^{\max}$, $k_\omega^{\max}$, $\xi_\omega^{\min}$ and $k_\omega^{\min}$, we can find a solution for the trade-off between

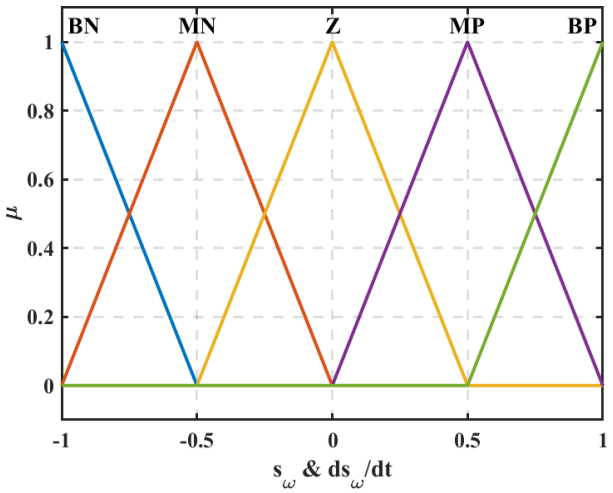


**Fig. 3** Membership function of the inputs $s_\omega$ and $\dot{s}_\omega$

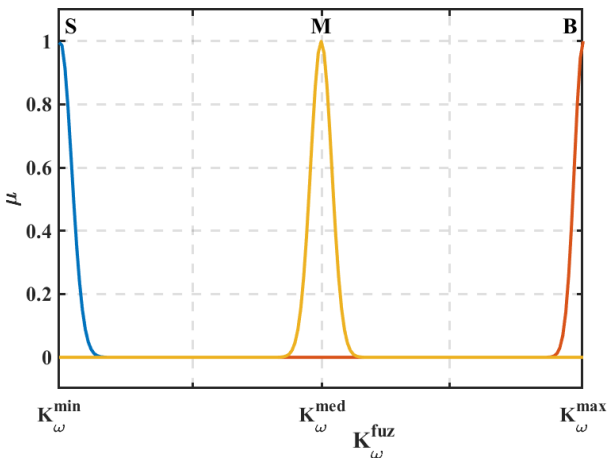


**Fig. 4** Membership function of the output $k_\omega^{fuz}$

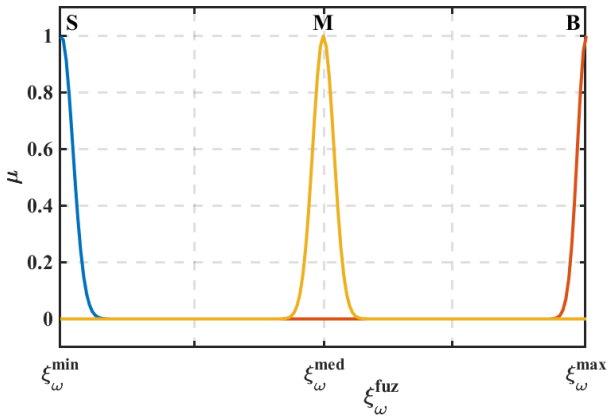


**Fig. 5** Membership function of the output $\xi_\omega^{fuz}$

robustness and chattering reduction. Finally, the two-dimensional inference matrix, which groups the rules governing the online adaptation of both parameters, $k_\omega^{fuz}$ and $\xi_\omega^{fuz}$, is shown in Table 1.

## 5 Experimental results

The effectiveness of the fuzzy adaptive sliding mode control for induction motor speed control has been experimentally verified. An experimental test platform has been done in various operating conditions to verify the proposed control method analysis. The machine parameters are given in Table 2. The experimental test setup exhibited in Fig. 6 has been processed using a dSPACE DS1104 R&D board with TMS320F240 DSP and Control Desk experiment software. As shown in Fig. 6, the experimental platform consists of a 250W three-phase wound rotor induction motor fed by a three-phase inverter (SEMIKRON) and a 250W DC generator fed by a resistance serving for generating load torque. The driver adaptation designed based on ULN2803 serves to amplify the PWM signals generated by the dSpace1104 card board from a 0-5V logic level to a 0-15V logic level. The parameters chosen of the FASMC speed controller are listed as follows: $k_\omega = 0.5$, $\xi_\omega = 1.65$, $k_\omega^{\min} = k_\omega$, $k_\omega^{\text{med}} = 0.9$, $k_\omega^{\max} = 1.3$, $\xi_\omega^{\min} = \xi_\omega$, $\xi_\omega^{\text{med}} = 1.92$, $\xi_\omega^{\max} = 2.2$.

**Table 1** Fuzzy rules of the fuzzy adaptation system

| $k_\omega^{fuz}$, $\xi_\omega^{fuz}$ | | $s_\omega$ | | | | |
|---|---|---|---|---|---|---|
| | | BN | MN | Z | MP | BP |
| $\dot{s}_\omega$ | BN | B | B | B | M | S |
| | MN | B | M | M | S | S |
| | Z | M | M | S | M | M |
| | MP | M | S | M | M | B |
| | BP | S | S | B | B | B |

**Table 2** Nominal IM parameters values

| Parameter | Value |
|---|---|
| Rated power $P_n$ | 250 W |
| Line-line voltage $V_n$ | 398 V |
| Rated current $I_n$ | 0.86 A |
| Rated speed $\Omega_n$ | 1350 rpm |
| Number of pole pairs $P$ | 2 |
| Stator resistance $R_s$ | 39.36 Ω |
| Rotor resistance $R_r$ | 35.6015 Ω |
| Stator inductance $L_s$ | 3.6076 H |
| Rotor inductance $L_r$ | 3.6076 H |
| Magnetizing inductance $L_m$ | 3.233 H |
| Inertia moment of motor $J$ | 0.0013 kg/m$^2$ |
| Friction coefficient $f_c$ | 0.0047 Nm s/rad |

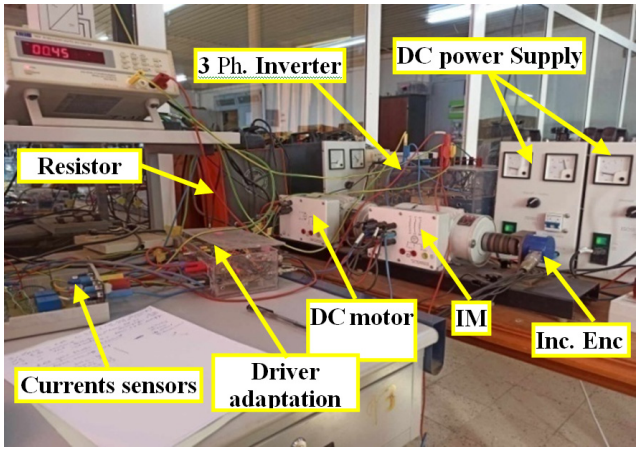


(a)

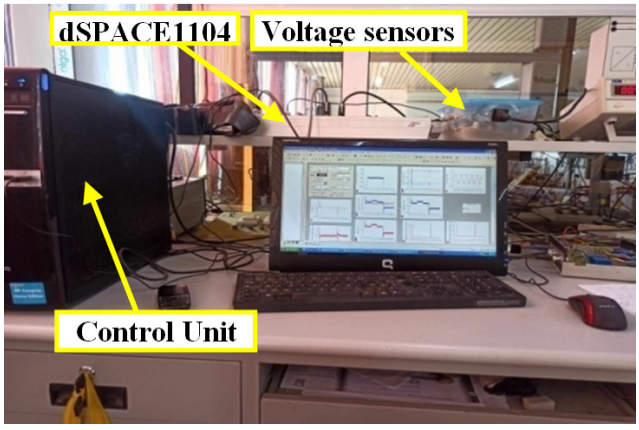


(b)

**Fig. 6** Photograph view of experimental setup (a) IM drive system (b) PC, dSPACE 1104 and sensors

A test with both transient and steady state operating conditions for the induction machine drive is implemented to illustrate the efficiency of the proposed fuzzy adaptive sliding mode control. The test involves a step change in speed reference from 1200 rpm to −1200 rpm, with the reference speed reversing at 6.4 s. We start the IM drive system with a constant load of 0.35 Nm, apply an additive load torque of 0.5 Nm at $t$ = 2.4 s, and eliminate it at $t$ = 4.4 s.

The performance of the IM drive using the proposed fuzzy adaptive SMC control scheme under this operating test is depicted in Fig. 7 (a)-(e). The rotor speed and the rotor fluxes ($\varphi_{dr}$, $\varphi_{qr}$) are depicted in Fig. 7 (a) and (b), respectively. Fig. 7 (a) and (b) clearly shows that the proposed FASMC scheme can achieve good tracking performance with high precision and accuracy even with load torque disturbance variation. In Fig. 7 (a), the speed response of the proposed fuzzy adaptive sliding mode control is observed to present better tracking characteristics and more robustness against speed reference reversals (minimal rising time, minimum undershoot against load torque application, with no overshoot).The proposed scheme maintains the $d$-axis rotor flux level constant at its nominal value, highlighting a proper cross-coupling and an accurate field orientation of $\varphi_{qr}$ = 0. Fig. 7 (c)-(e) shows the $dq$-axis stator currents, electromagnetic torque and estimated load torque value, and stator phase current. Fig. 8 also depicts the values of the adaptive parameters ($k_\omega^{fuz}$, $\xi_\omega^{fuz}$) of the switching function. Fig. 9 illustrates the waveform of the phase "$a$" stator voltage generated by the inverter feeding the Induction Motor (IM) drive. It is clear that the stator voltage waveform is rich in harmonics due to its discontinuous behavior and the chosen switching frequency of the PWM signals. This harmonic content has significant implications for the motor's performance, including increased losses and torque ripple.

To further demonstrate the superiority of the proposed FASMC in terms of control performance, comparative experience with classical sliding mode control has been done. The comparison tests consist of the following:

- Test 1: Comparison of speed responses between the classical SMC and the proposed FASMC under the same nominal operating conditions already carried out.
- Test 2: The robustness of the controllers is tested under main uncertainty conditions. In the first case, the control system is operated with a 50% increase of the inertia moment $J$, and in the second case, the IM drive is operated under a 50% increase of the rotor resistance $R_r$.

For the first test, Fig. 10 illustrates the speed responses of the proposed FASMC and the classical SMC. In Fig. 10, it can be observed that the proposed FASMC controller outperforms the classical SMC in tracking performance and exhibits greater robustness and overall effectiveness.

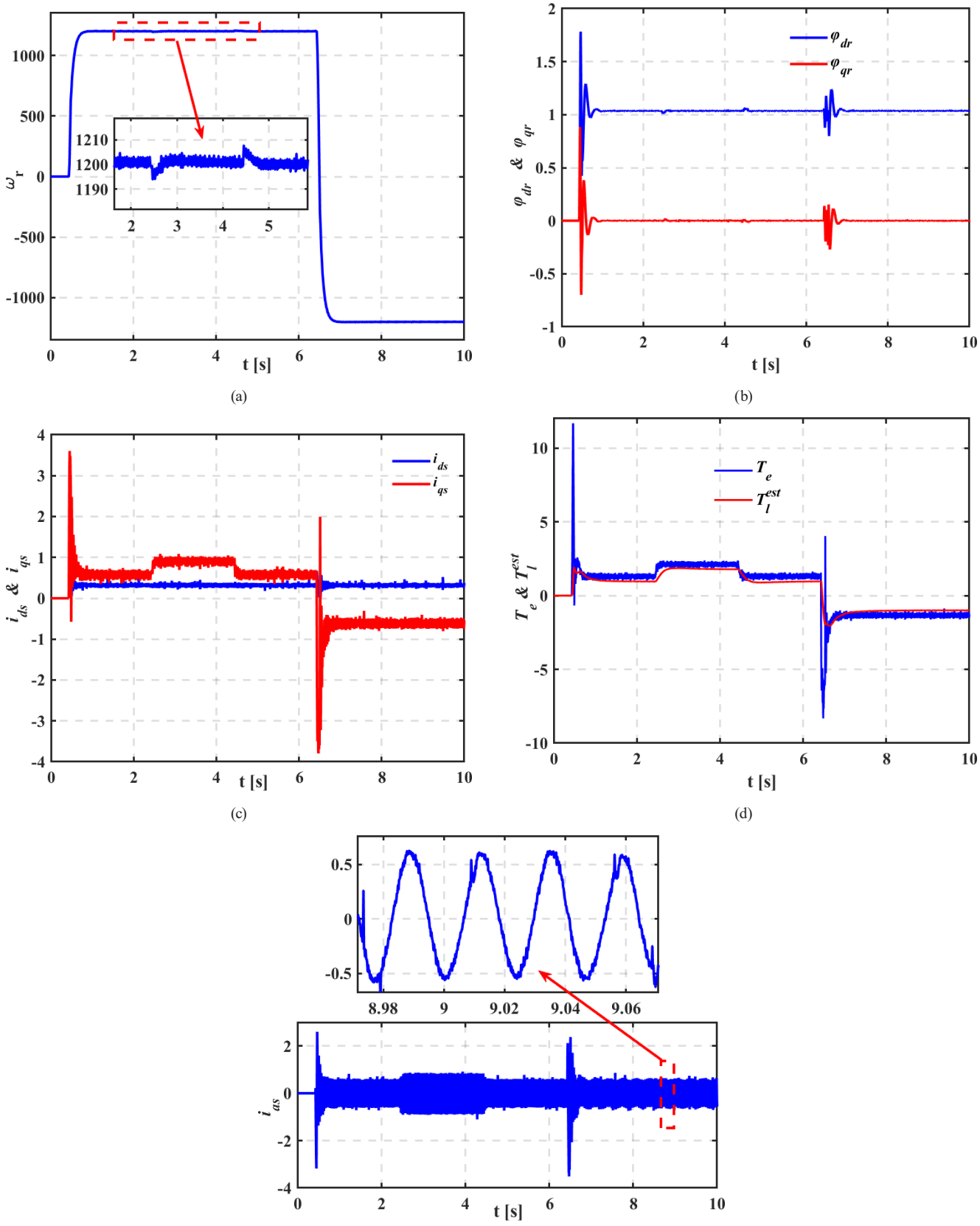


**Fig. 7** Experimental results of the proposed FASMC IM drive: (a) Speed, (b) $\varphi_{dr}$ &$\varphi_{qr}$, (c) $i_{ds}$ & $i_{qs}$, (d) $T_e$ & $T_l^{est}$, (e) $i_{as}$

In terms of settling time and rise time, it can be seen that the speed response using classical SMC provides an overshoot of 38 rpm at start-up and over 70 rpm during speed reversal. Additionally, it shows an undershoot of 10 rpm when

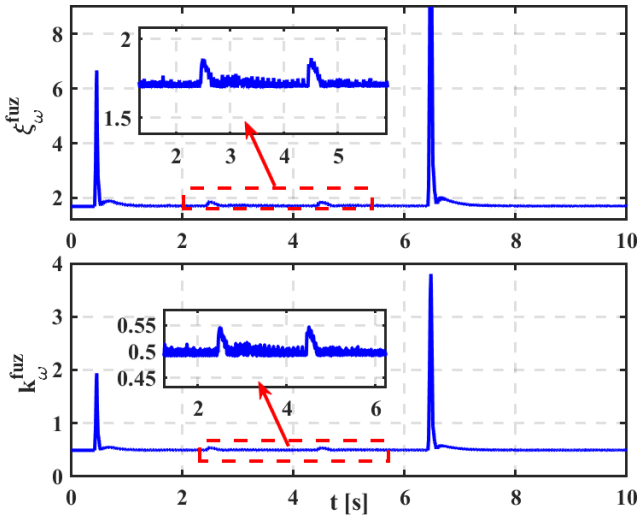


**Fig. 8** Parameters of switching function: ($k_\omega^{fuz}$, $\xi_\omega^{fuz}$)

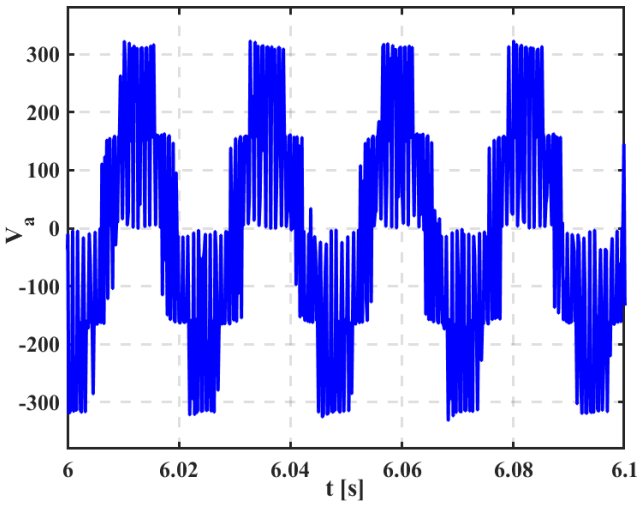


**Fig. 9** Supply voltage waveform of the phase "*a*"

load torque is increased. The suggested FASMC, on the other hand, doesn't overshoot when starting up or switching speeds. When the load torque is applied, it only undershoots slightly, and it recovers its speed much faster than the classical SMC.

Figs. 11 and 12 illustrate the speed responses of the SMC and the FASMC for the second test. Fig. 11 illustrates the system behavior when it operates under 50% increasing of inertia moment, whereas Fig. 12 shows the robustness of controllers against rotor resistance increasing. From Figs. 11 and 12, it can be clearly observed that the hybrid controller achieves superior tracking performance with minimal deviation, even under transient operating conditions and parameter uncertainty, compared to the classical SMC, which exhibits larger deviations and slower convergence to the desired speed. Table 3 presents a comparative analysis between the speed controllers, taking into account several performance indicators. In addition, the phase plane of

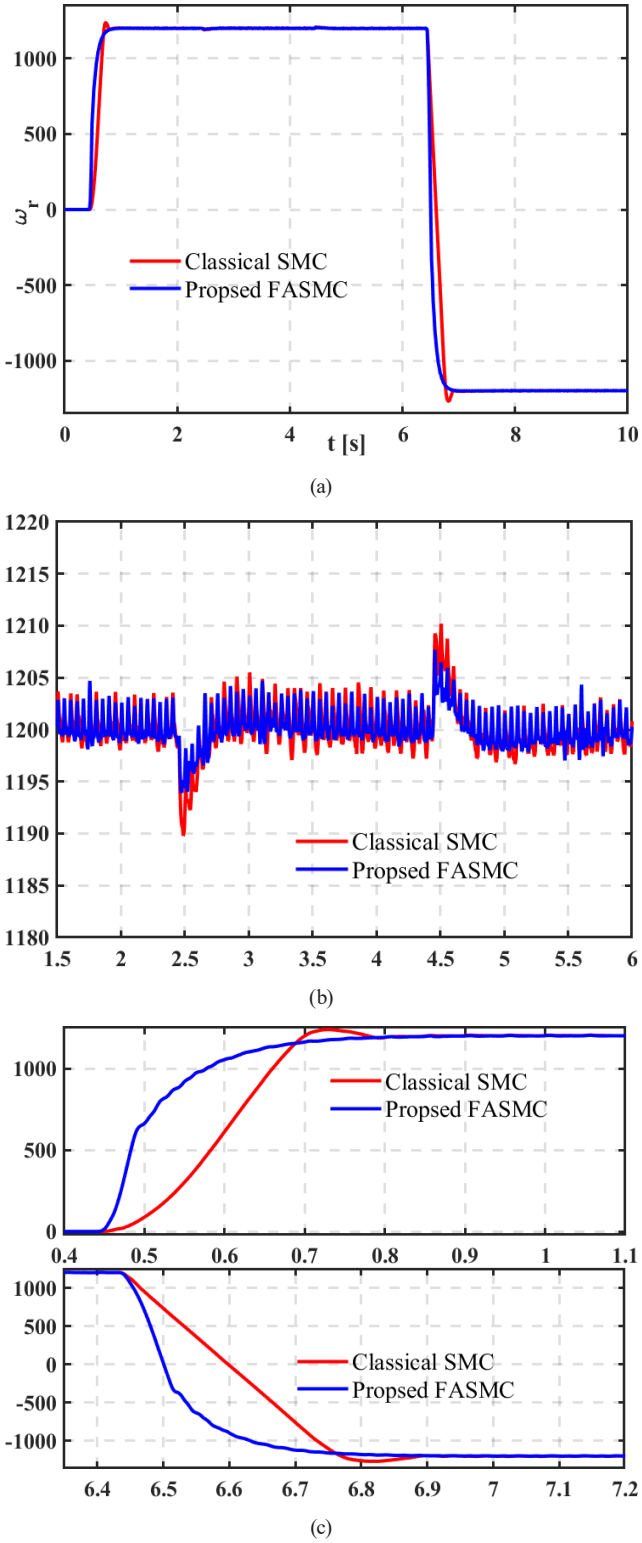


**Fig. 10** Speed responses comparison between classical SMC and FASMC control: (a) Speed, (b) Speed zoom at load application and (c) Speed zoom at motor starting and speed reversal time

state trajectories for the two controllers, classical SMC and fuzzy adaptive SMC (FASMC), are shown in Fig. 13. These phase planes, which represent the speed error time-derivative against the speed error, offer a visual illustration of the

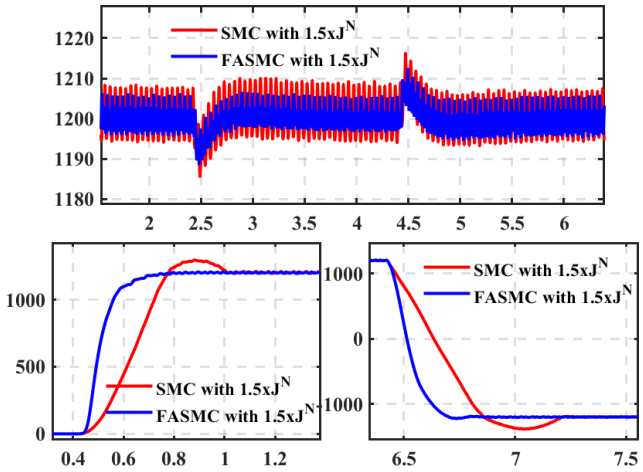


**Fig. 11** Performance comparison between classical SMC and FASMC under 50% increase of $J$

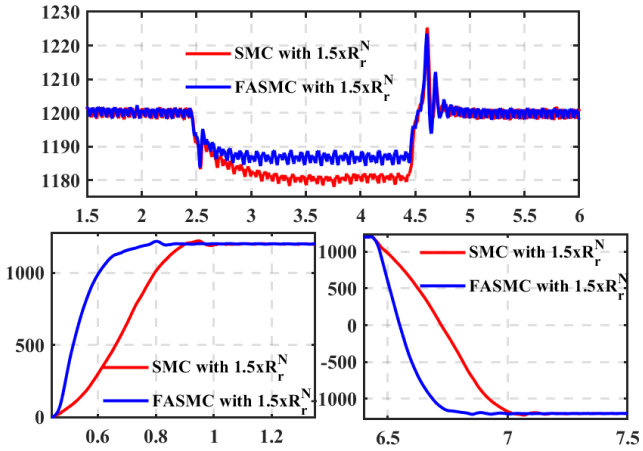


**Fig. 12** Performance comparison between classical SMC and FASMC under 25% increase of $R_r$

**Table 3** Comparison between FASMC and SMC

| | Classical SMC | Proposed FASMC |
|---|---|---|
| Robustness | Medium | High |
| Chattering reduction | Medium | Good |
| Rising-time | 0.183 | 0.154 |
| Steady-state time | 0.36 | 0.29 |
| IAE | 0.2093 | 0.1193 |
| ISE | 0.1956 | 0.0904 |
| ITSE | 0.0957 | 0.0409 |
| ITAE | 0.1309 | 0.0810 |

system's dynamic behavior and highlight the effectiveness of the two control strategies in reaching the desired equilibrium point. In the phase plane of classical SMC, it can be clearly seen that the state trajectories exhibit high-frequency oscillation around the sliding surface, which indicates an important chattering stress. In contrast, the phase plane for FASMC reveals a smoother and more stable convergence

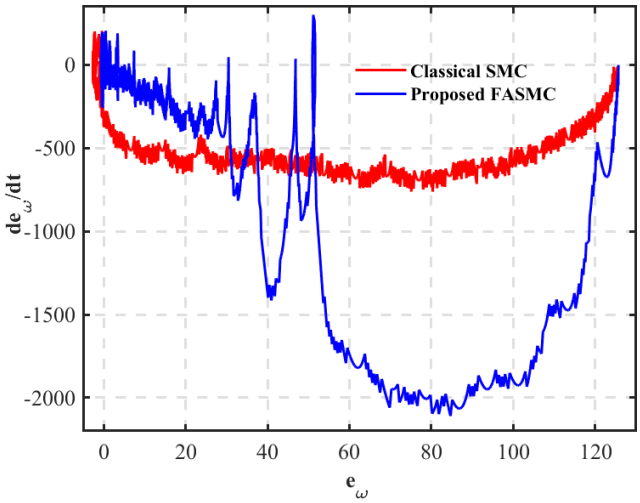


**Fig. 13** Phase trajectories of SMC and FASMC for IM control drive

of the state trajectories toward the sliding surface. This adaptive mechanism significantly provides smoother control actions and improved system performance. Moreover, the switching control terms for both the classical SMC and FASMC, i.e., Eqs. (24) and (39), against the sliding surface are illustrated in Figs. 14 and 15, respectively. In Figs. 14 and 15, it is evident that the switching control action in classical SMC exhibits a saturation form, where the control signal alternates between a maximum and minimum value depending on the variation of the sliding surface. On the other hand, the switching control action in FASMC is more dynamic and adaptive, as it continuously tunes the switching gain and boundary layer thickness based on the system's operating conditions. By this dynamically tuning process, FASMC achieves smoother control actions, effectively reducing chattering while maintaining robust performance.

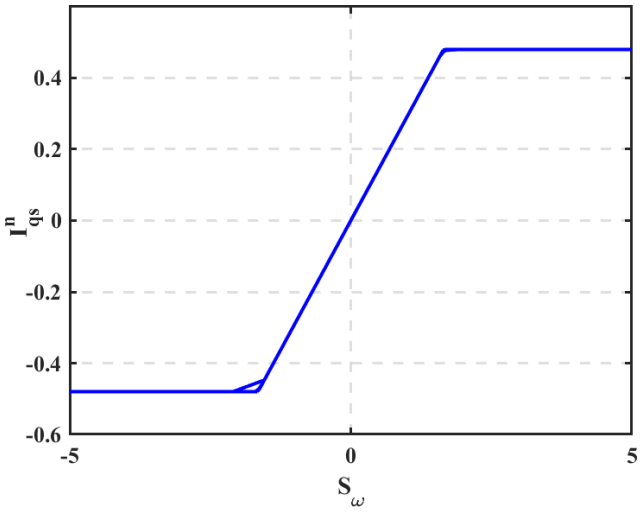


**Fig. 14** Switching control action of classical SMC against sliding surface

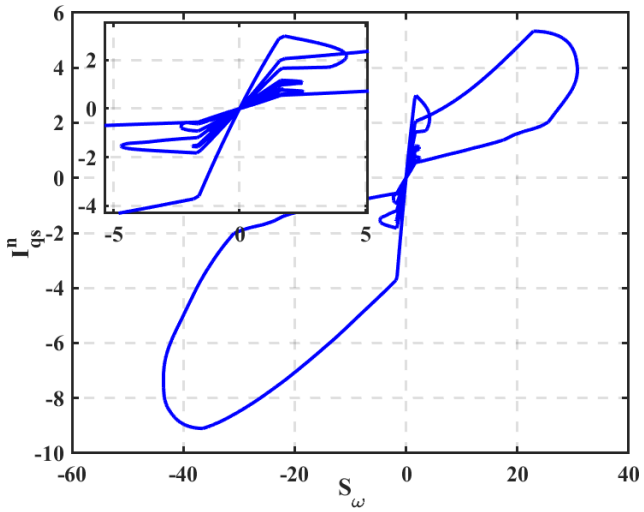


**Fig. 15** Switching control action of the proposed FASMC against sliding surface

## 6 Conclusion

In this paper, we proposed a fuzzy adaptive sliding mode controller for speed control of the IM drive system to enhance the control performances under different operation conditions, modes, and load variations and reduce chattering issues. Firstly, we developed a sliding mode control based on the indirect field-oriented control architecture. Then, a fuzzy adaptive controller was designed to adjust the two parameters of the switching control law in the classical SMC, based on the error and its derivative variation. The adaptation method involves adjusting the switching control action's gains based on the transient and steady-state conditions of the IM drive system, as well as the system's position relative to the sliding surface. An experimental setup using dSPACE1104 successfully verified the effectiveness of the proposed adaptive fuzzy sliding mode control of the IM drive during both steady and transient states. The results make it clear that the suggested fuzzy adaptive sliding mode controller (FASMC) does a good job of controlling IM speed, with high accuracy and convergence at steady-state conditions and when the load increases and decreases. With these potential benefits, the proposed Fuzzy Adaptive Sliding Mode Control (FASMC) stands out as a very useful and adaptable control method that can handle the difficulties of different electric motor drives and a large number of dynamic systems. Its important mix of robustness and adaptability makes it a good choice for complicated, nonlinear, and uncertain systems, guaranteeing dependable and effective dynamic performance in a wide range of settings. Robotic systems, power electronic converters, self-driving automobiles, aerospace technologies, and many more industrial applications can benefit from the proposed FASMC's ability to address modern control problems by combining the best aspects of fuzzy logic and sliding mode control.

## References

[1] Wach, P. "Dynamics and Control of Electrical Drives", Springer, 2011. ISBN 978-3-642-20221-6
https://doi.org/10.1007/978-3-642-20222-3

[2] Veltman, A., Pulle, D. W. J., De Doncker, R. W. "Fundamentals of Electrical Drives", Springer, 2016. ISBN 978-3-319-29408-7
https://doi.org/10.1007/978-3-319-29409-4

[3] Quang, N. P., Dittrich, J.-A. "Vector Control of Three-Phase AC Machines: System Development in the Practice", Springer, 2015. ISBN 978-3-662-46914-9
https://doi.org/10.1007/978-3-662-46915-6

[4] Mohan, N., Raju, S. "Analysis and Control of Electric Drives: Simulations and Laboratory Implementation", John Wiley & Sons, Inc., 2020. ISBN 9781119584537
https://doi.org/10.1002/9781119584575

[5] De Doncker, R. W., Pulle, D. W. J., Veltman, A. "Advanced Electrical Drives: Analysis, Modeling, Control", Springer, 2020. ISBN 978-3-030-48979-3
https://doi.org/10.1007/978-3-030-48977-9

[6] Trzynadlowski, A. M. "The Field Orientation Principle in Control of Induction Motors", Springer, 1993. ISBN 978-0-7923-9420-4
https://doi.org/10.1007/978-1-4615-2730-5

[7] Vas, P. "Sensorless vector and Direct Torque control", Oxford University Press, 1998. ISBN 9780198564652
https://doi.org/10.1093/oso/9780198564652.001.0001

[8] Wai, R.-J. "Adaptive Sliding-Mode Control for Induction Servomotor Drives", IEE Proceedings - Electric Power Applications, 147(6), pp. 553–562, 2000.
https://doi.org/10.1049/ip-epa:20000628

[9] Lin, C.-M., Hsu, C.-F. "Adaptive Fuzzy Sliding-Mode Control for Induction Servomotor Systems", IEEE Transactions on Energy Conversion, 19(2), pp. 362–368, 2004.
https://doi.org/10.1109/TEC.2003.821859

[10] Wai, R.-J., Lin, C.-M., Hsu, C.-F. "Adaptive Fuzzy Sliding-Mode Control for Electrical Servo Drive", Fuzzy Sets and Systems, 143(2), pp. 295–310, 2004.
https://doi.org/10.1016/S0165-0114(03)00199-4

[11] Saghafinia, A., Wooi Ping, H., Nasir Uddin, M. "Fuzzy sliding mode control based on boundary layer theory for chattering-free and robust induction motor drive", The International Journal of Advanced Manufacturing Technology, 71(1), pp. 57–68, 2014.
https://doi.org/10.1007/s00170-013-5398-7

[12] Utkin, V. I. "Sliding Mode Control Design Principles and Applications to Electric Drives", IEEE Transactions on Industrial Electronics, 40(1), pp. 23–36, 1993.
https://doi.org/10.1109/41.184818

[13] Slotine, J.-J., Li, W. "Applied Nonlinear Control", Prentice-Hall. Inc., 1991. ISBN 0-13-040890-5

[14] Utkin, V., Guldner, J., Shi, J. "Sliding mode control in electromechanical systems", CRC Press, 2017. ISBN 9781315218977 https://doi.org/10.1201/9781420065619

[15] Sira-Ramírez, H. "Sliding mode control: The Delta-Sigma Modulation Approach", Springer, 2015. ISBN 978-3-319-17256-9 https://doi.org/10.1007/978-3-319-17257-6

[16] Liu, J. Wang, X. "Advanced Sliding Mode Control for Mechanical Systems: Design, Analysis and MATLAB Simulation", Springer, 2012. ISBN 978-3-642-20906-2 https://doi.org/10.1007/978-3-642-20907-9

[17] Sun, C., Gong, G., Yang, H. "Sliding Mode Control with Adaptive Fuzzy Immune Feedback Reaching Law", International Journal of Control, Automation and Systems, 18(2), pp. 363–373, 2020. https://doi.org/10.1007/s12555-019-0285-0

[18] Amieur, T., Taibi, D., Bechouat, M., Kahla, S., Sedraoui, M. "Fuzzy Sliding Mode with adaptive gain control for nonlinear MIMO systems", Romanian Journal of Information Technology and Automatic Control, 32(3), pp. 95–108, 2022. https://doi.org/10.33436/v32i3y202208

[19] Jamoussi, K., Ouali, M., Chrif-Alaoui, L., Benderradji, H., El Hajjaji, A. "Robust Sliding Mode Control Using Adaptive Switching Gain for Induction Motors", International Journal of Automation and Computing, 10(4), pp. 303–311, 2013. https://doi.org/10.1007/s11633-013-0725-x

[20] Nurettin, A., İnanç, N. "Design of a robust hybrid fuzzy super-twisting speed controller for induction motor vector control systems", Neural Computing and Applications, 34, pp. 19863–19876, 2022. https://doi.org/10.1007/s00521-022-07519-4

[21] Cherifi, D., Miloud, Y. "Hybrid Control Using Adaptive Fuzzy Sliding Mode Control of Doubly Fed Induction Generator for Wind Energy Conversion System", Periodica Polytechnica Electrical Engineering and Computer Science, 64(4), pp. 374–381, 2020. https://doi.org/10.3311/PPee.15508

[22] Itouchene, H., Boudries, Z., Amrane, F. "Improved Power Control Based Variable Speed Wind-Turbine DFIG under Hard Work Conditions: Application of Sliding Mode Theory", Periodica Polytechnica Electrical Engineering and Computer Science, 68(4), pp. 392–412, 2024. https://doi.org/10.3311/PPee.36760

[23] Feng, H., Jiang, J., Chang, X., Yin, C., Cao, D., Yu, H., Li, C., Xie, J. "Adaptive sliding mode controller based on fuzzy rules for a typical excavator electro-hydraulic position control system", Engineering Applications of Artificial Intelligence, 126, 107008, 2023. https://doi.org/10.1016/j.engappai.2023.107008

[24] Ullah, A., Ullah, S., Rahman, T. U., Sami, I., Rahman, A. U., Alghamdi, B., Pan, J. "Enhanced wind energy conversion system performance using fast smooth second-order sliding mode control with neuro-fuzzy estimation and variable-gain robust exact output differentiator", Applied Energy, 377, 124364, 2025. https://doi.org/10.1016/j.apenergy.2024.124364

[25] Veysi, M., Soltanpour, M. R. "Voltage-Base Control of Robot Manipulator Using Adaptive Fuzzy Sliding Mode Control", International Journal of Fuzzy Systems, 19(5), pp. 1430–1443, 2017. https://doi.org/10.1007/s40815-016-0234-5

[26] Aichi, B., Kendouci, K. "A Novel Switching Control for Induction Motors Using a Robust Hybrid Controller that Combines Sliding Mode with PI Anti-Windup", Periodica Polytechnica Electrical Engineering and Computer Science, 64(4), pp. 392–405, 2020. https://doi.org/10.3311/PPee.15661

[27] Yang, Y., Wang, Y., Zhang, W., Li, Z., Liang, R. "Design of Adaptive Fuzzy Sliding-Mode Control for High-Performance Islanded Inverter in Micro-Grid", Energies, 15(23), 9154, 2022. https://doi.org/10.3390/en15239154

[28] Saghafinia, A., Ping, H. W., Uddin, M. N., Gaeid, K. S. "Adaptive Fuzzy Sliding-Mode Control Into Chattering-Free IM Drive", IEEE Transactions on Industry Applications, 51(1), pp. 692–701, 2015. https://doi.org/10.1109/TIA.2014.2328711

[29] Mishra, R. N., Mohanty, K. B. "Development and implementation of induction motor drive using sliding-mode based simplified neuro-fuzzy control", Engineering Applications of Artificial Intelligence, 91, 103593, 2020. https://doi.org/10.1016/j.engappai.2020.103593

[30] Kiyyour, B., Laggoun, L., Salhi, A., Naimi, D., Boukhalfa, G. "Improvement DTC for Induction Motor Drives Using Modern Speed Controllers Tuning by PSO Algorithm", Periodica Polytechnica Electrical Engineering and Computer Science, 67(3), pp. 249–259, 2023. https://doi.org/10.3311/PPee.21000

[31] Boukhalfa, G., Belkacem, S., Chikhi, A., Bouhentala, M. "Fuzzy-second order sliding mode control optimized by genetic algorithm applied in direct torque control of dual star induction motor", Journal of Central South University, 29(12), pp. 3974–3985, 2022. https://doi.org/10.1007/s11771-022-5028-3

[32] Baek, S., Baek, J., Han, S. "An Adaptive Sliding Mode Control With Effective Switching Gain Tuning Near the Sliding Surface", IEEE Access, 7, pp. 15563–15572, 2019. https://doi.org/10.1109/ACCESS.2019.2894911

[33] Sacchi, N., Incremona, G. P., Ferrara, A. "Neural Network-Based Practical/Ideal Integral Sliding Mode Control", IEEE Control Systems Letters, 6, pp. 3140–3145, 2022. https://doi.org/10.1109/LCSYS.2022.3182814

[34] Roy, S., Baldi, S., Fridman, L. M. "On adaptive sliding mode control without a priori bounded uncertainty", Automatica, 111, 108650, 2020. https://doi.org/10.1016/j.automatica.2019.108650

[35] Wan, L, Chen, G, Sheng, M, Zhang, Y, Zhang, Z. "Adaptive chattering-free terminal sliding-mode control for full-order nonlinear system with unknown disturbances and model uncertainties", International Journal of Advanced Robotic Systems, 17(3), 1729881420925295, 2020. https://doi.org/10.1177/1729881420925295

[36] Elsisi, M., Bazmohammadi, N., Guerrero, J. M., Ebrahim, M. A. "Energy management of controllable loads in multi-area power systems with wind power penetration based on new supervisor fuzzy nonlinear sliding mode control", Energy, 221, 119867, 2021. https://doi.org/10.1016/j.energy.2021.119867

[37] Zhong, G., Wang, C., Dou, W. "Fuzzy adaptive PID fast terminal sliding mode controller for a redundant manipulator", Mechanical Systems and Signal Processing, 159, 107577, 2021. https://doi.org/10.1016/j.ymssp.2020.107577

[38] Madebo, M. M. "Neuro-Fuzzy-Based Adaptive Sliding Mode Control of Quadrotor UAV in the Presence of Matched and Unmatched Uncertainties", IEEE Access, 12, pp. 117745–117760, 2024. https://doi.org/10.1109/ACCESS.2024.3447474

[39] Dat, N. T., Van Kien, C., Anh, H. P. H. "Advanced adaptive neural sliding mode control applied in PMSM driving system", Electrical Engineering, 105(5), pp. 3255–3262, 2023. https://doi.org/10.1007/s00202-023-01874-8

[40] Hou, S., Fei, J., Chu, Y., Chen, C. "Experimental Investigation of Adaptive Fuzzy Global Sliding Mode Control of Single-Phase Shunt Active Power Filters", IEEE Access, 7, pp. 64442–64449, 2019. https://doi.org/10.1109/ACCESS.2019.2917020

[41] Chiang, C.-J., Chen, Y.-C. "Neural network fuzzy sliding mode control of pneumatic muscle actuators", Engineering Applications of Artificial Intelligence, 65, pp. 68–86, 2017. https://doi.org/10.1016/j.engappai.2017.06.021

[42] Fei, J., Chen, Y., Liu, L., Fang, Y. "Fuzzy Multiple Hidden Layer Recurrent Neural Control of Nonlinear System Using Terminal Sliding-Mode Controller", IEEE Transactions on Cybernetics, 52(9), pp. 9519–9534, 2022. https://doi.org/10.1109/TCYB.2021.3052234

[43] Nguyen-Vinh, Q., Pham-Tran-Bich, T. "Sliding mode control of induction motor with fuzzy logic observer", Electrical Engineering, 105(5), pp. 2769–2780, 2023. https://doi.org/10.1007/s00202-023-01842-2